Electronic Supplementary Material (ESI) for Inorganic Chemistry Frontiers.


# Supplementary Information

# Coral-like $ZnFe_2O_4$-ZnO heterojunction architectures: synthesis and enhanced sensing properties for triethylamine

Tianye Yang[a], Xiaodong Yang[c], Mingming Zhu[b], Hongwei Zhao[a*] and Mingzhe Zhang[b*]

[a]School of Mechanical and Aerospace Engineering, Jilin University, Changchun 130025, People's Republic of China, E-mail**:** hwzhao@jlu.edu.cn

[b]State key laboratory of Superhard materials, Jilin University, Changchun 130012, People's Republic of China, E-mail: zhangmz@jlu.edu.cn

[c]School of Mechanical Engineering, Jilin Engineering Normal University, Changchun 130052, People's Republic of China.

### 1.1 Sensor structure

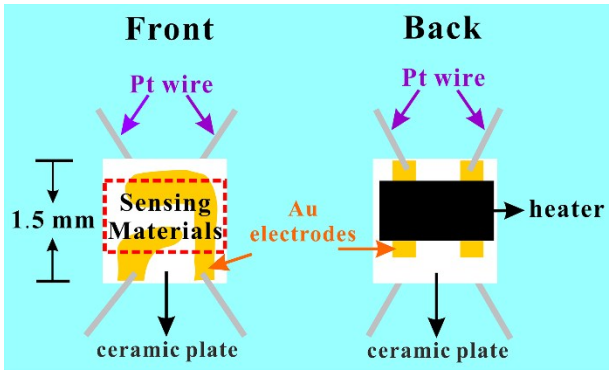


**Fig. S1** The schematic diagram of the as-fabricated gas sensor structure.

### 1.2 Synthesis of Materials

All the chemical reagents involved in the experiments zinc nitrate hexahydrate ($Zn(NO_3)_2$•$6H_2O$), iron(III) nitrate nonahydrate ($Fe(NO_3)_3$•$9H_2O$), iron(II) sulphate heptahydrate ($Fe(SO_4)_2$•$7H_2O$), terephthalic acid (1,4-benzenedicarboxylic acid, $HOOCC_6H_4COOH$, PTA), and carbamide ($CO(NH_2)_2$) were analytical pure and purchased without further purification. Deionized water (18.2 MΩ•cm) was used for all the experiments.

#### 1.2.1 Pure ZnO sample

Typically, 0.0016 mol $Zn(NO_3)_2 \cdot 6H_2O$, 0.02 mol $CO(NH_2)_2$, 0.001 mol PTA and 20 mL deionized water were mixed and stirred for 30 min and then transferred into a small vial with about 20 mL capacity, maintained in an oven at 95 $^oC$ for 24 h. The vial was cooled down to room temperature naturally. The white precipitate was then collected and washed with anhydrous alcohol and deionized water for three times by centrifugalization and dried at 60 $^oC$ in air. The ZnO sample was obtained by annealing the precursor at 500 $^oC$ for 2 h with heating rate 5 $^oC\ min^{-1}$.

#### 1.2.2 Pure $ZnFe_2O_4$ sample

Generally, 0.0016 mmol $Zn(NO_3)_2 \cdot 6H_2O$, 0.0032 mmol $Fe(SO_4)_2 \cdot 7H_2O$, 0.02 mol $CO(NH_2)_2$, 0.001

mol PTA and 20 mL deionized water were mixed and stirred for 30 min and then transferred into a small vial with 20 mL capacity, maintained in an oven at 95 °C for 24 h. And then the vial was cooled down to room temperature naturally. The red-brown precipitate was collected and washed with anhydrous alcohol and deionized water for several times and dried in air at 60 °C. The pure $ZnFe_2O_4$ sample was obtained by annealing the precursor at 450 °C for 2 h with heating rate 2 °C/min.

### 1.2.3 Structure and Morphology

The structure and morphology information are shown in Fig. S2. Figure S2a and S2b show the XRD patterns of pure ZnO and pure $ZnFe_2O_4$. The patterns exhibit clear and strong diffraction peaks that are in good agreement with the hexagonal structure ZnO pattern (JCPDS card No. 36-1451) shown in Fig. S2b and typical cubic $ZnFe_2O_4$ pattern (JCPDS card No. 22-1012) shown in Fig. S2b. Figure S2c and S2d indicate that the morphology of pure ZnO sample and $ZnFe_2O_4$ sample. It can be observed that the morphology of ZnO sample is similar with the heterojunction sample.

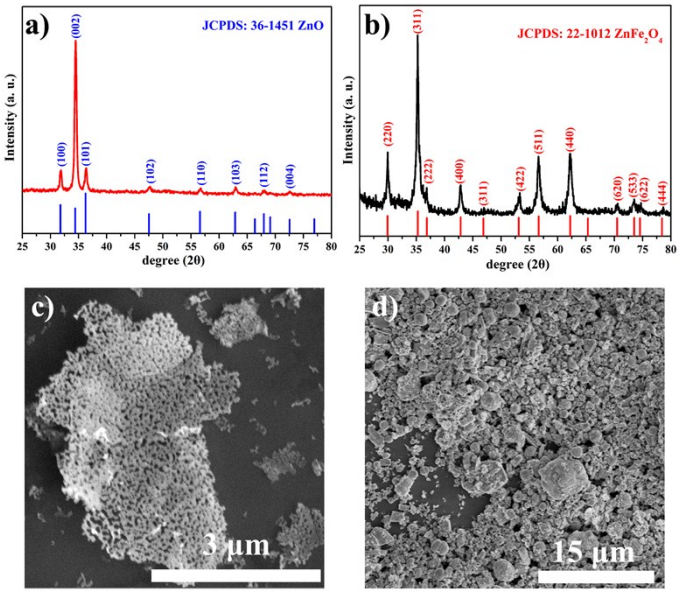


**Fig. S2** (a) XRD pattern of pure ZnO sample. (b) XRD pattern of pure $ZnFe_2O_4$ sample. (c) SEM image of pure ZnO sample. (d) SEM image of pure $ZnFe_2O_4$ sample.

### 1.3 UV-vis spectra investigation

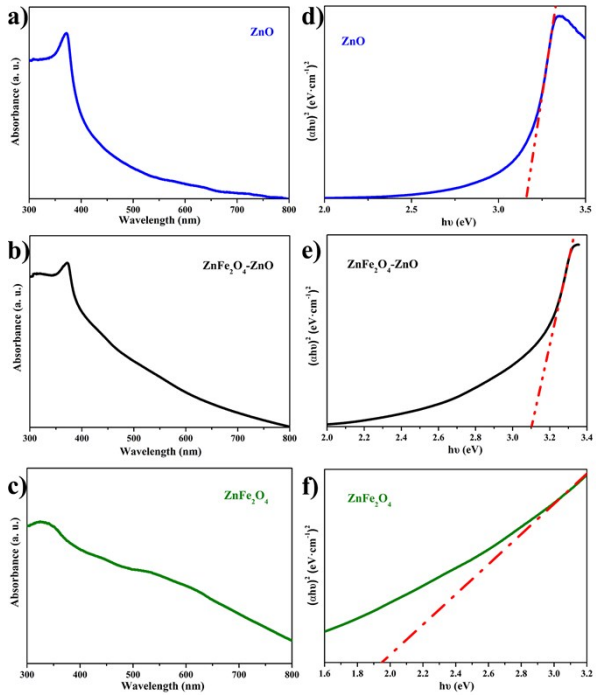


**Fig. S3** (a-c) UV-vis spectra of pure ZnO, $ZnFe_2O_4$-ZnO heterojunction, and pure $ZnFe_2O_4$sample. (d-f) Tauc plots to determine the band-gap energies ($E_g$) of the ZnO, $ZnFe_2O_4$-ZnO, and $ZnFe_2O_4$ sample.

The UV absorption spectra of the pure ZnO sample, $ZnFe_2O_4$-ZnO heterojunction sample and pure $ZnFe_2O_4$ sample are illustrated in Fig. S3a, S3b and S3c respectively. It is observed that all samples exhibit strong ultraviolet absorption. The Tauc method is used to calculate the band gap energy values from a linear extrapolation of the plots of the $(Ahν)^n$ vs. the photon energy (hν), as shown in Fig. S3d, S3e and S3f. The ZnO and $ZnFe_2O_4$ are typical n type semiconductors and the n value is set at 2.The obtained band gap values were 3.16 eV for the pure ZnO sample, 3.10 eV for the $ZnFe_2O_4$-ZnO heterojunction sample and 1.95 eV for the pure $ZnFe_2O_4$ sample, which are consistent with the previous reports.[1]. The bandgap value of heterojunction sample is slightly smaller than the pure ZnO sample, which indicates that the $ZnFe_2O_4$ (Eg=1.95 eV) is grown together with the pristine ZnO sample. The UV-vis spectra results indicate that the heterojunction structure is formed in the sample and it is consistent with the HRTEM results.

Further, the conduction band (CB) bottom and the valence band (VB) tops of ZnO and $ZnFe_2O_4$ can be calculated by the formulas:

$$E_{VB} = \chi - E_e + 0.5E_g \quad (1)$$

$$E_{CB} = E_{VB} - E_g \quad (2)$$

where $\chi$ is the absolute electronegativity of ZnO (5.79 eV) and $ZnFe_2O_4$ (5.86 eV), $E_e$ is the energy of free electrons on the hydrogen scale (4.5 eV) and $E_g$ is the band gap of ZnO (3.16 eV) and $ZnFe_2O_4$ (1.95 eV).[2, 3] The CB and VB of ZnO and $ZnFe_2O_4$ are calculated to be −0.29 eV, 2.87 eV and 0.385 eV, 2.335 eV respectively. As a result, a heterogeneous structure between $ZnFe_2O_4$ and ZnO materials can be schematically described in Fig. 8 of the manuscript.

### 1.4 Growth mechanism

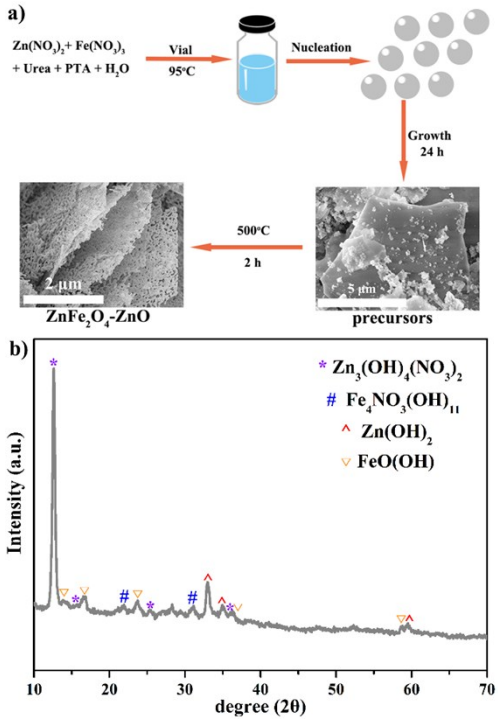


**Fig. S4** (a) The schematic diagram of growth process of the coral-like $ZnFe_2O_4$-ZnO heterojunction architectures. (b) The XRD pattern of the as-synthesized precursor.

Based on abovementioned tests in the manuscript, a plausible growth mechanism of the as-synthesized coral-like $ZnFe_2O_4$-ZnO mesoprous morphology is proposed and a schematic illustration of growth process is shown in Fig. S4. As depicted in Fig. S4a, at first, a certain amount of $Zn(NO_3)_2$, $Fe(NO_3)_3$, PTA and urea was dissolved in 20 mL deionized water. Then, the solution was transferred into a vial and maintained at 95°C in an oven for 24 h. The $Zn^{2+}$ and $Fe^{3+}$ ions in the solution were reacted with $OH^-$ ions which were provided by the hydrolysis of urea to form $Zn(OH)_2$ and $Fe(OH)_3$ crystal nuclei respectively. The $Fe(OH)_3$ species were further oxidized by the dissolved oxygen in the solution to FeOOH. The abovementioned reaction were represented as equation (3)-(7).

$$CO(NH_2)_2 + H_2O \rightarrow 2NH_3 + CO_2 \quad (3)$$

$$NH_3 + H_2O \rightarrow NH_4^+ + OH^- \quad (4)$$

$$Zn^{2+} + 2OH^- \rightarrow Zn(OH)_2 \quad (5)$$

$$Fe^{3+} + 3OH^- \rightarrow Fe(OH)_3 \quad (6)$$

$$2Fe^{3+} + 2OH^- + O_2 \rightarrow 2FeOOH \quad (7)$$

$$2FeOOH + Zn(OH)_2 \rightarrow 2ZnFe_2O_4 + 2H_2O \quad (8)$$

$$Zn(OH)_2 \rightarrow ZnO + H_2O \quad (9)$$

In addition, the PTA had some special characteristics including two carboxyl groups, a high structuring effect and low steric hindrance.[4] All these properties of PTA made it easily combine with the metal ions to form chelate and well-crystallized compounds with specific morphology were obtained. In this study, the $Zn^{2+}$ ions and $Fe^{3+}$ ions in alkaline circumstance grew into sheet-like morphology precursors with the assistance of PTA and the XRD pattern of the precursor was shown in Fig. S4b. The as-synthesized precursor was further annealed at 500 °C and the FeOOH species reacted with $Zn(OH)_2$ species to form $ZnFe_2O_4$ species. Due to excess amount of $Zn^{2+}$ ions, redundant $Zn(OH)_2$ species further dehydrated to form ZnO under calcination. And the mesoporous structure could be derived from the dehydration process under thermal treatment. Finally, the $ZnFe_2O_4$-ZnO mesoporous heterojunction architectures were successfully obtained. The proposed reactions were illustrated in

equation (8) and (9).

### 1.5 Gas sensing performance

The TEA sensing performance, transient response presentation of pure $ZnFe_2O_4$ sample and pure ZnO sensor to 50 ppm TEA, is illustrated in Fig. S5. The Fig. S5a indicates that the pure ZnO based sensor exhibits a response/recovery speed of 0.9 s/51 s and a response value of 7.7 at operating temperature 200 °C. Figure S5b shows the pure $ZnFe_2O_4$ based sensor exhibits a response/recovery speed of 3.7 s/112 s and a response value of 11.4 at operating temperature 180 °C.

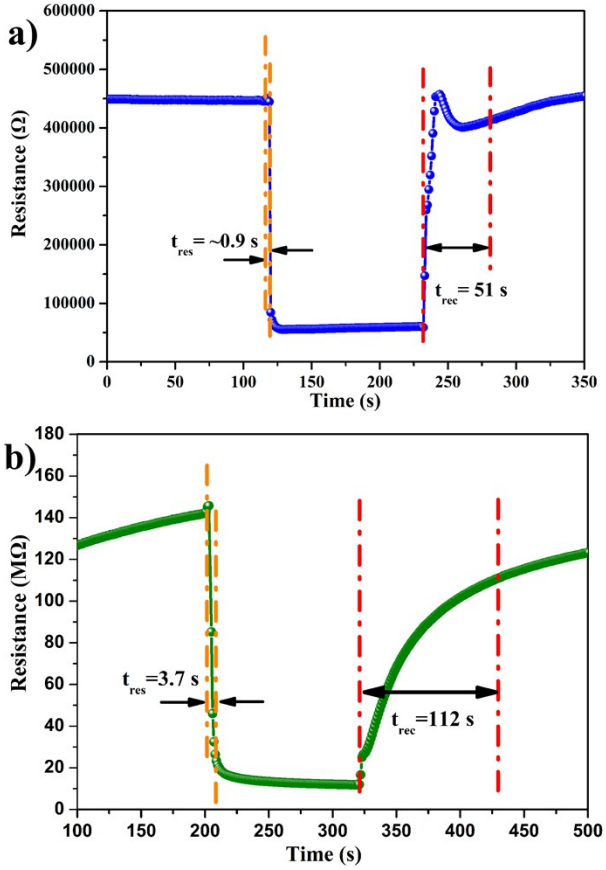


**Fig. S5** (a) The transient response presentation of pure ZnO based sensor to 50 ppm TEA. (b) The transient response presentation of pure $ZnFe_2O_4$ based sensor to 50 ppm TEA.

The stability of the sensor is another parameter to its practical applications. To verify the stability of the coral-like $ZnFe_2O_4$-ZnO mesoporous heterojunction sensor, the gas response evolution is investigated under 50 ppm TEA at operating temperature 240 °C for 30 days, as show in Fig. S6. No obviously decrease in gas response was observed over the testing period, indicating the good stability of the sensor.

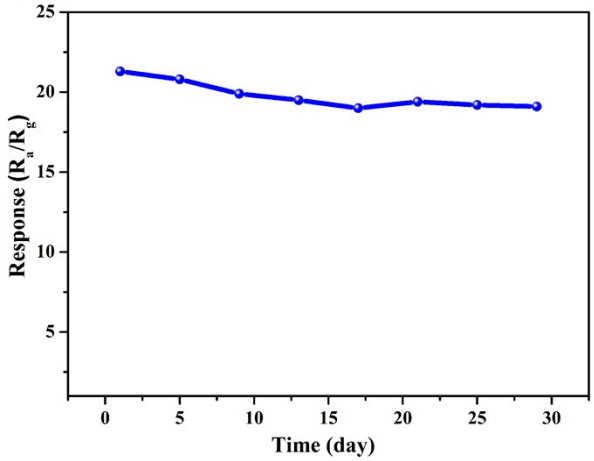


**Fig. S6** Long-term stability of the coral-like $ZnFe_2O_4$-ZnO mesoporous heterojunction sensor to 50 ppm of TEA at 240 °C.

## Reference


1. J. H. Kim, J. H. Kim, J.-W. Jang, J. Y. Kim, S. H. Choi, G. Magesh, J. Lee and J. S. Lee, Awakening Solar Water-Splitting Activity of $ZnFe_2O_4$ Nanorods by Hybrid Microwave Annealing, *Advanced Energy Materials*, 2015, **5**, 1401933.
2. P. Hu, C. Chen, J. Song and Z. Tang, Efficient visible-light photocatalysis of ZIF-derived mesoporous $ZnFe_2O_4$/ZnO nanocomposite prepared by a two-step calcination method, *Mater. Sci. Semicond. Process.*, 2018, **77**, 40-49.
3. Y. Zhou, S. Fang, M. Zhou, G. Wang, S. Xue, Z. Li, S. Xu and C. Yao, Fabrication of novel $ZnFe_2O_4$/BiOI nanocomposites and its efficient photocatalytic activity under visible-light irradiation, *Journal of Alloys and Compounds*, 2017, **696**, 353-361.
4. C. Daiguebonne, N. Kerbellec, K. Bernot, Y. Gérault, A. Deluzet and O. Guillou, Synthesis, Crystal Structure, and Porosity Estimation of Hydrated Erbium Terephthalate Coordination Polymers, *lnorg. Chem.*, 2006, **45**, 5399-5406.